Theoretical Simulations of GNSS Reflections from Bare and Vegetated Soils

R. Giusto[1], L. Guerriero[2], S. Paloscia[3], N. Pierdicca[1], A. Egido[4], N. Floury[5]

1 DIET - Sapienza Univ. of Rome, Rome
2 DISP - University of Tor Vergata, Rome
3 CNR/IFAC, Sesto Fiorentino
4 Starlab, Barcelona
5 CNR/IFAC, Rome

Content

- Introduction: the Leimon project
- Simulator description
  - ✓ General formulation
  - ✓ SW Structure
  - ✓ Models and algorithms
- Simulator output examples
- Simulator validation during Leimon

Leimon Project

ESA funded the LEIMON project aiming at

- **evaluating the potential of GNSS signals for remote sensing of land bio-geophysical parameters, through a ground based experimental campaign (see previous presentation)**
- **developing a simulator to theoretically explain experimental data and predict the capability of airborne and spaceborne GNSS-R systems for moisture and vegetation monitoring**

The Bistatic Radar Equation

The mean power of received signal vs. delay τ and frequency f is modeled by integral Bistatic Radar Equation which includes time delay domain response $\Lambda^2(\tau'-\tau)$ and Doppler domain response $S^2(f'-f)$ of the system (Zavorotny and Voronovich, 2000).

$$\left\langle \left| Y(\hat{\tau}, \hat{f}) \right|^2 \right\rangle = \frac{T_i^2 P_T \lambda^2}{(4\pi)^3} \int \frac{G_T G_R \Lambda^2(\tau'-\tau) S^2(f'-f)}{R_R^2 R_T^2} \sigma^0 dA$$

$\lvert Y \rvert^2$	**Processed signal power at the receiver vs. delay τ and frequency f.**
P_T	**The transmitted power of the GPS satellite.**
G_T, G_R	**The antenna gains of the transmitting and the receiving instrument.**
R_R, R_T	**The distance from target on the surface to receiving and transmitting antennas.**
T_i	**The coherent integration time used in signal processing.**
σ^o	**Bistatic scattering coefficient**
Λ^2	**The GPS correlation (triangle) function**
S^2	**The attenuation sinc function due to Doppler misalignment**
dA	**Differential area within scattering surface area A (the glistening zone).**

The BRE integration

Integrand variables are the coordinates defined on the surface

function of point scattering Doppler

function of point scattering delay

$$\left\langle \left| Y(\hat{\tau}, \hat{f}) \right|^2 \right\rangle = \frac{T_i^2 P_T \lambda^2}{(4\pi)^3} \int \frac{G_T G_R \Lambda^2(\tau' - \tau) S^2(f' - f)}{R_R^2 R_T^2} \sigma^0 dA$$

function of incidence direction

function of point looking direction wrt boresight

function of p
wrt RX and TX position

function of point bistatic angle (zenith and azimuth)

- In order to solve the integral we have to introduce the equations relating all those variables to the coordinates over the surface.

Local vs global frames

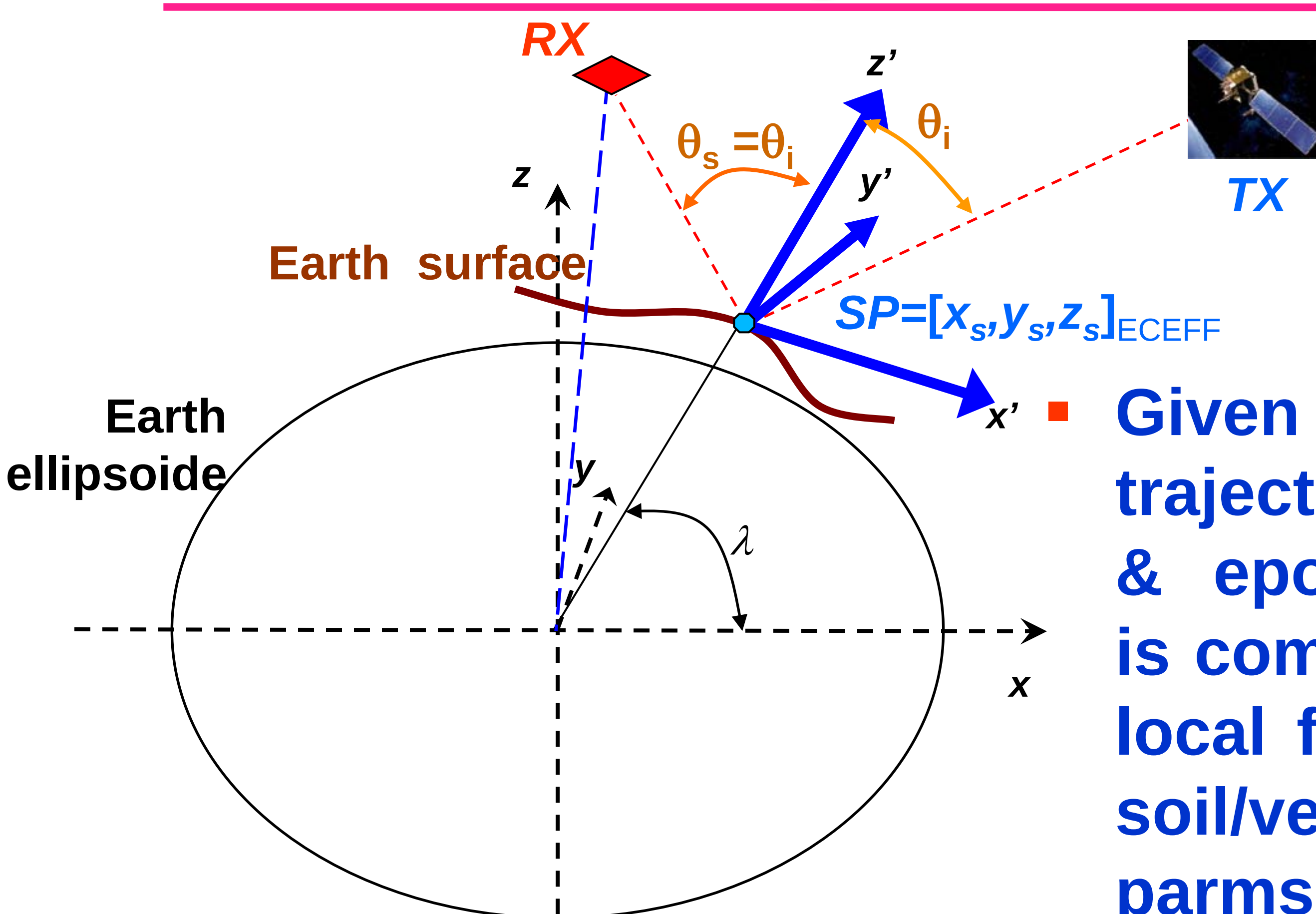

- Given RX and TX trajectory/velocity & epoch, integral is computed in the local frame, where soil/vegetation parms are defined

- Elliptic Earth approximation
- x'y'z' local frame centered in the specular point
- z' axes along the geodetic vertical
- x'z' plane coincident with the bistatic scattering plane

Simulator structure

- Bistatic $\sigma°$ of each point combined by BRE on a regular grid of delay and Doppler shift
- Receiver polarization accounted for by polarization synthesis using real antenna polarization
- Receiver antenna gain described as function of the point looking angle assuming a cosinusoidal pattern

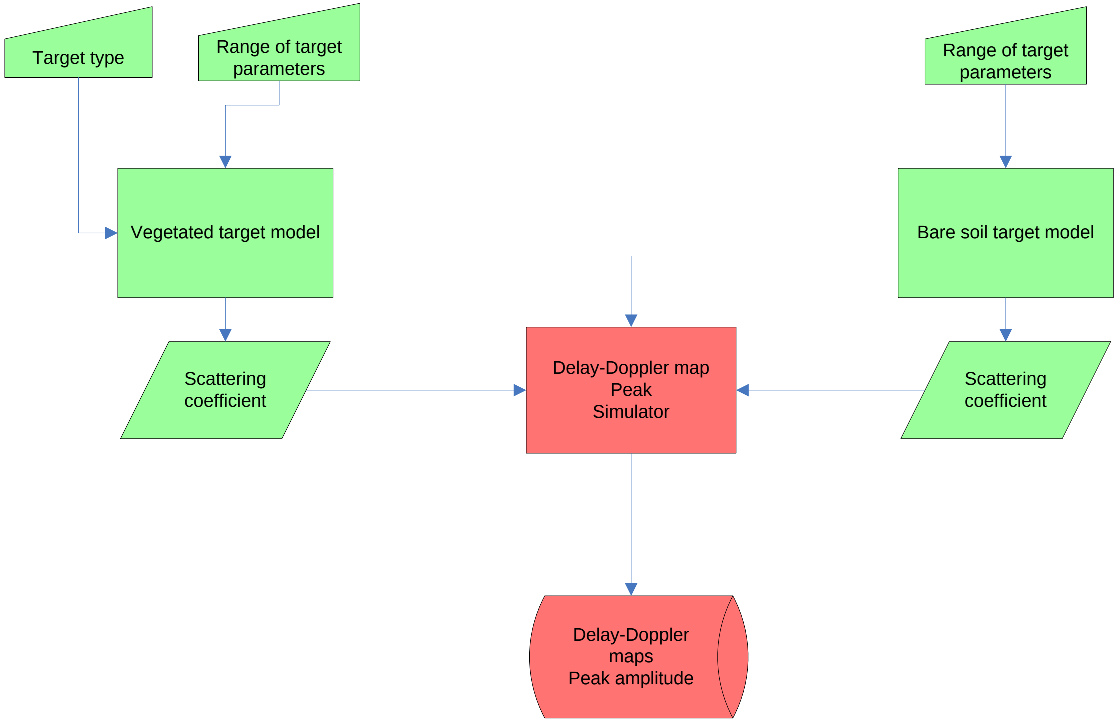

Electromagnetic modelling

Absent or homogeneous vegetation cover. ***Attenuation and multiple scattering by a discrete medium (Tor Vergata model)***

INCOHERENT component

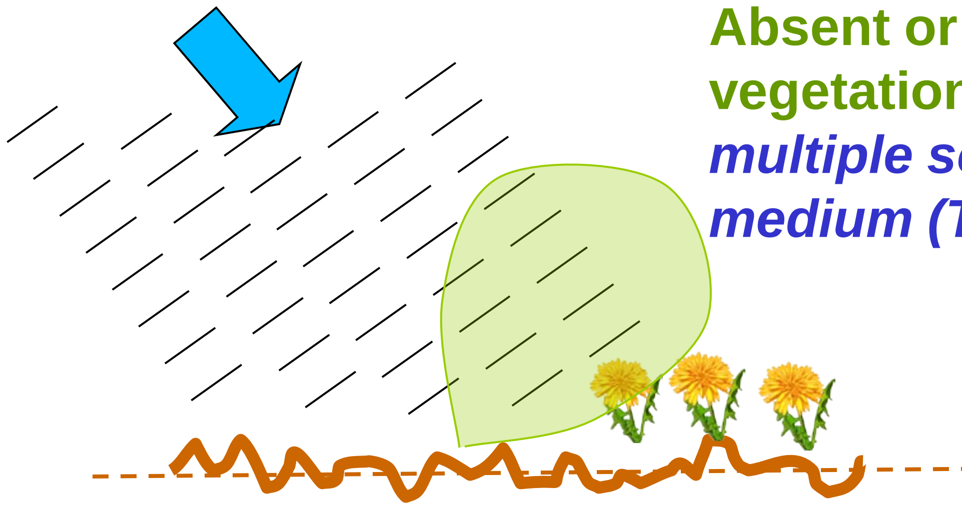

Indefinite mean surface plane with roughness at wavelength scale.
Bistatic scattering of locally incident plane waves by AIEM

Scattering of spherical wave by Kirchoff approxi. (Eom & Fung, 1988)

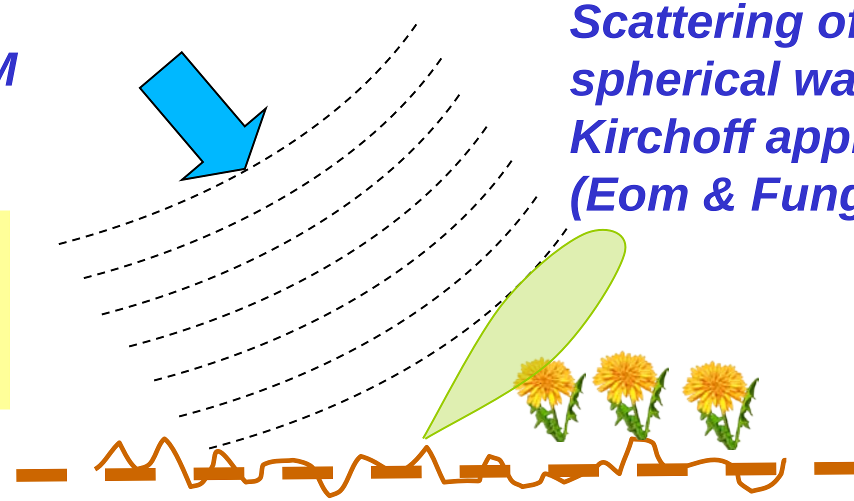

COHERENT component

Simulator output examples

Intermediate product:

- Scattering zenith angles
- isoDoppler and isorange lines on the surface
- RX antenna footprint
- Scattering azimuth angles

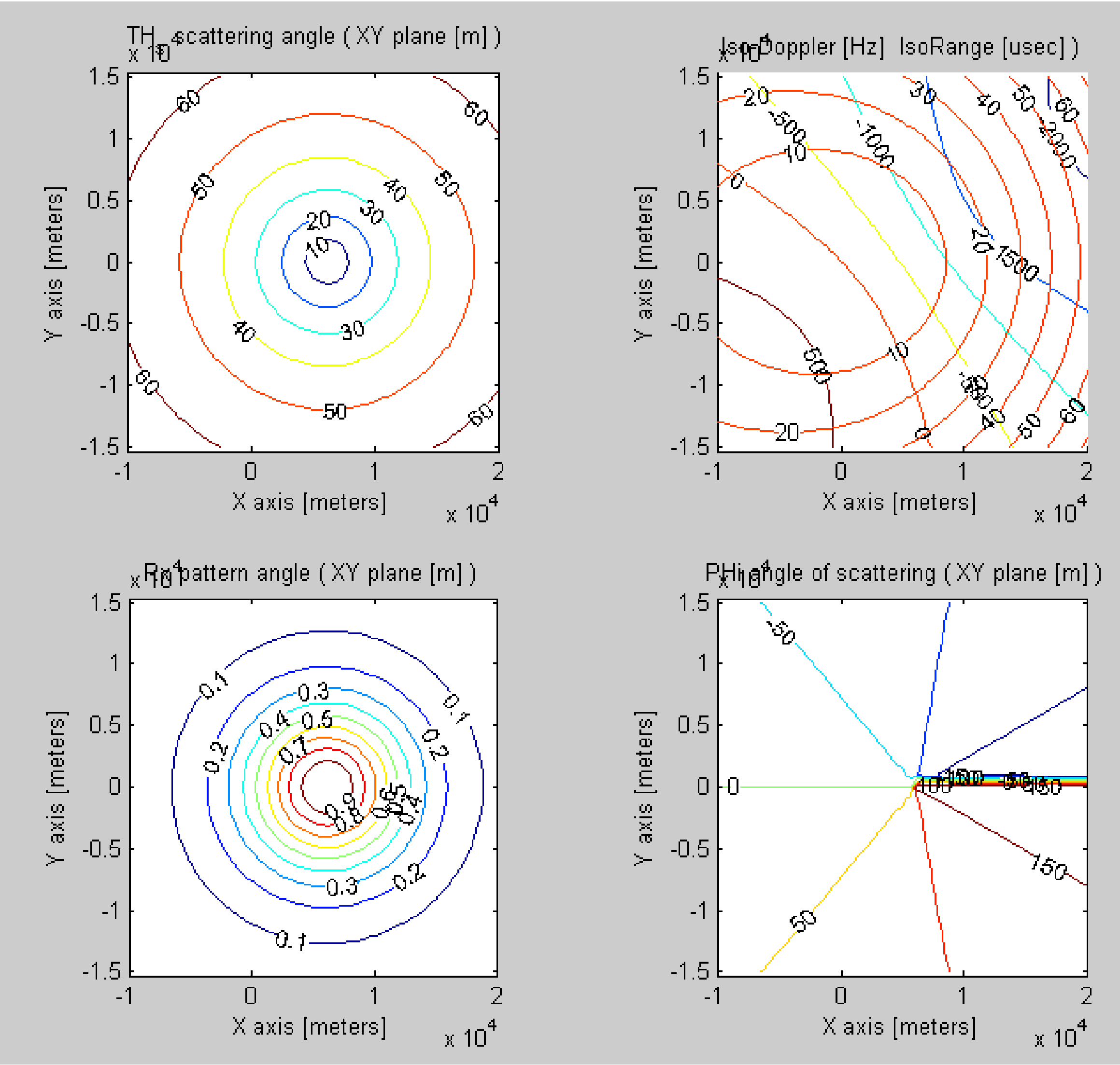

H_{RX}=10 km
V_{RX}=180 m/s
$Head_{RX}$=0°
HPBW=120°

AIEM vs scattering direction θ_s,φ_s

$\theta_i=31°$
$m_v=20$ %
$\sigma_z=1.5$ cm
$l=5$ cm
$H_{RX}=10$ km
HPBW=120°

- **Incoherent component RR & LR more spread**
- **Coherent component RR & LR focused around specular $\theta_s=31°$**

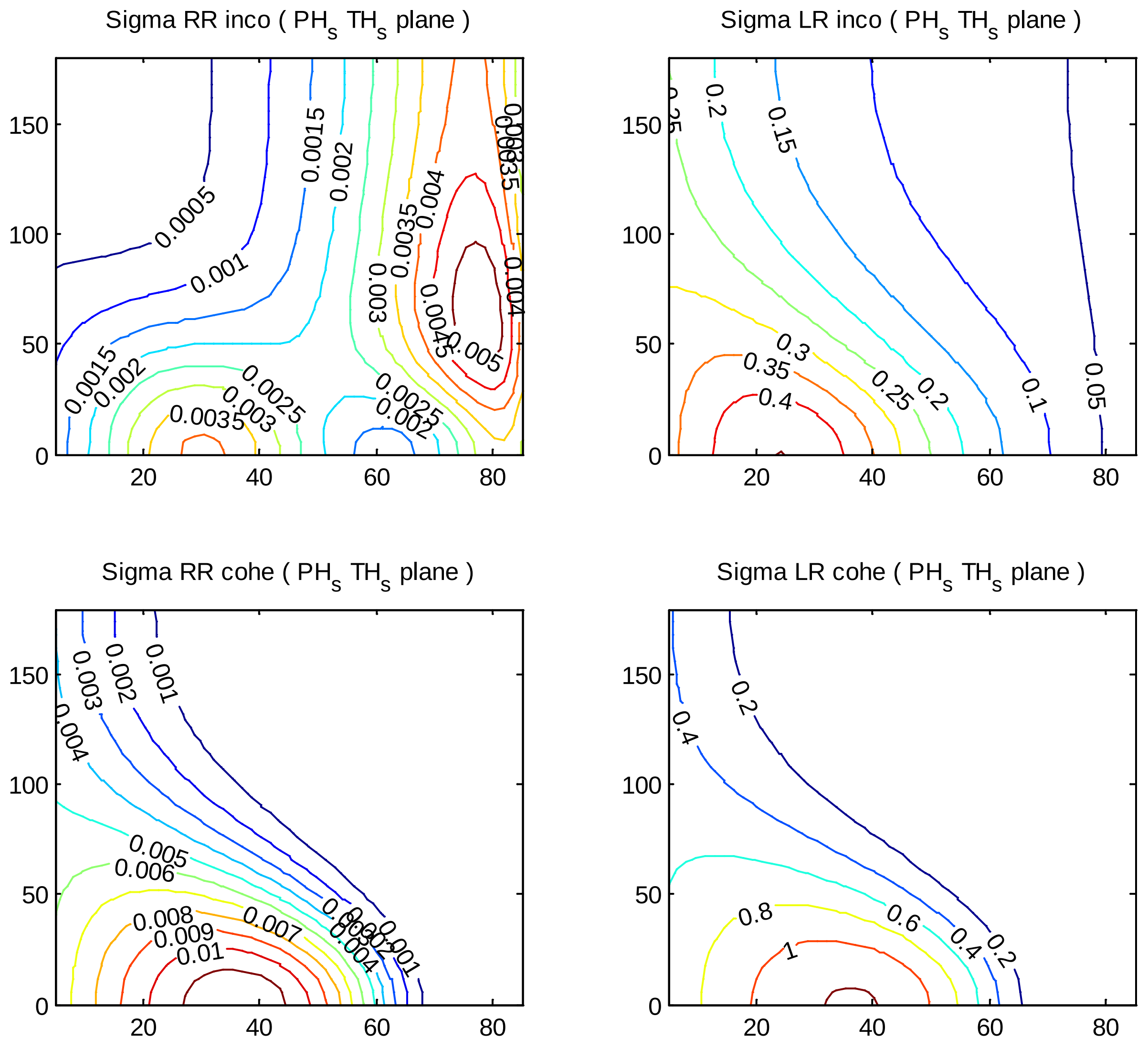

Bistatic scattering in local frame

$\theta_i=31°$
$m_v=20\ \%$
$\sigma_z=1.5$ cm
$l=5$ cm
$H_{RX}=10$ km
HPBW=120°

- Incoherent component RR & LR more spread
- Coherent component RR & LR focused around specular 0,0

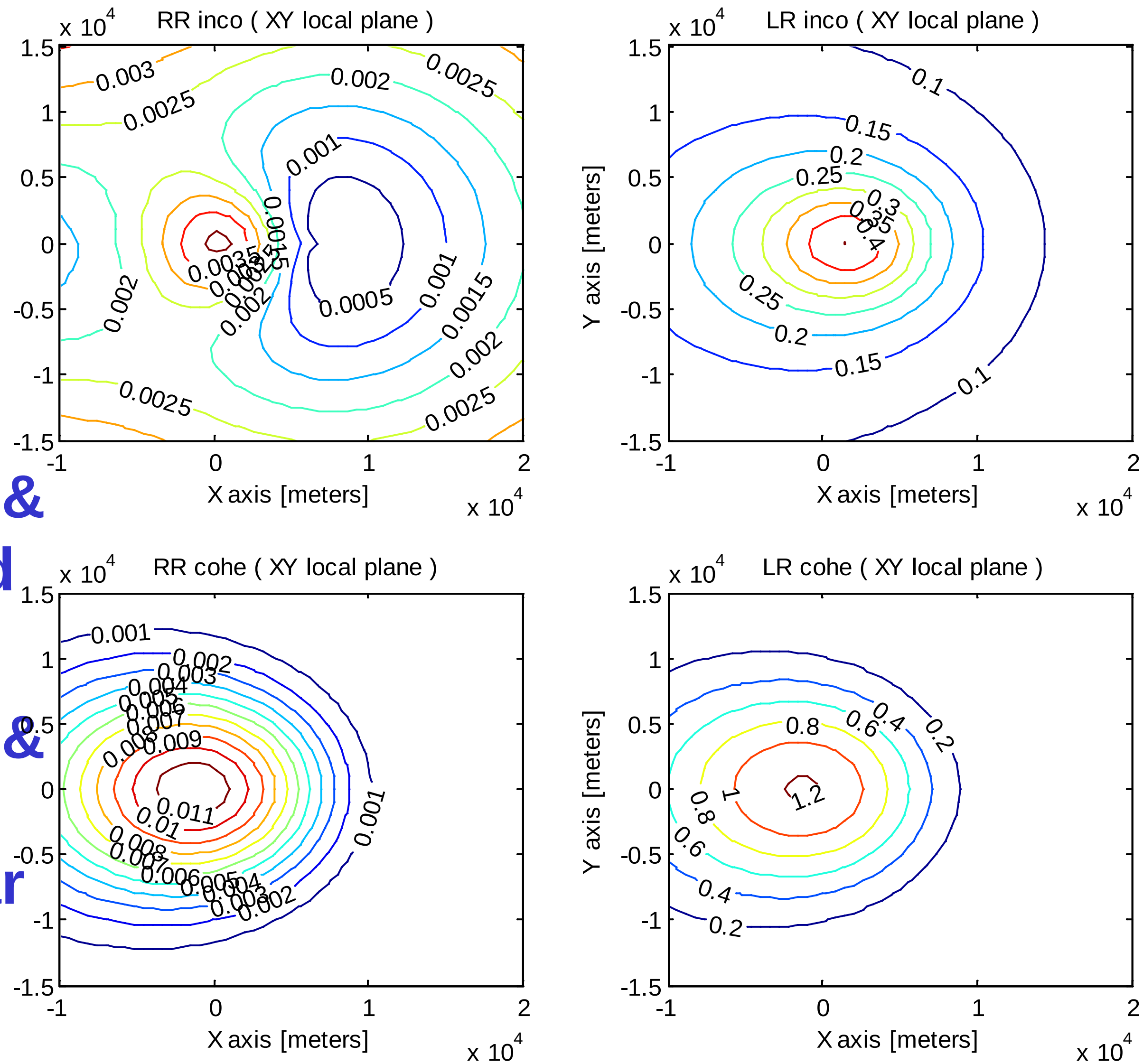

DDM output example

DDM's (delay on the horizontal axes, frequency on the vertical axes) for incoherent (top) and coherent (bottom) component at RHCP (left) and LHCP (right)

airbone incoherent

Spaceborne incoherent

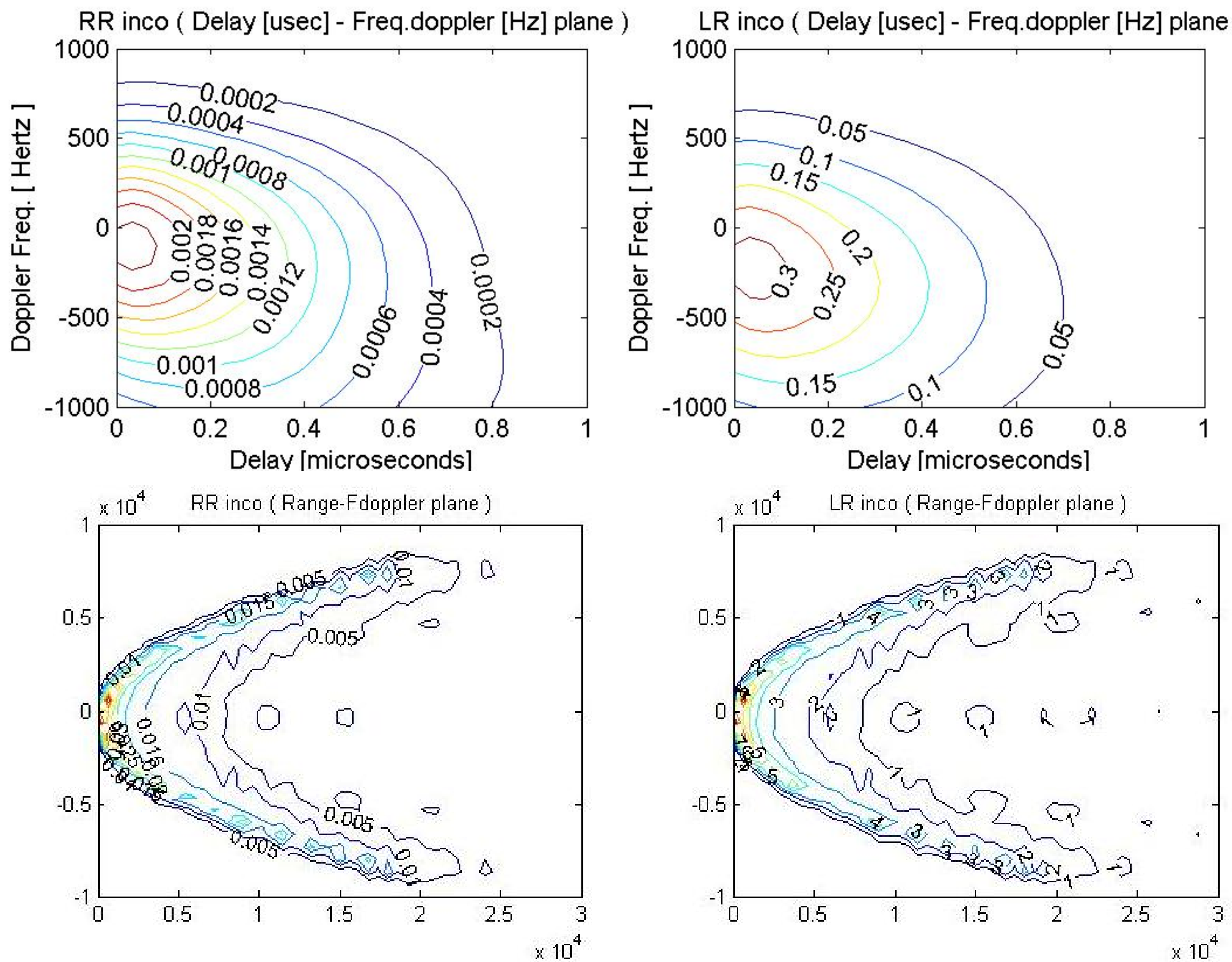

Peak power output example

m_v=20 %
σ_z=1.5 cm
l=5 cm
H_{RX}=10 km
V_{RX}=180 m/s
$Head_{RX}$=45°
HPBW=120°

- Coherent and incoherent RR & LR peak power as the satellite moves along the orbit

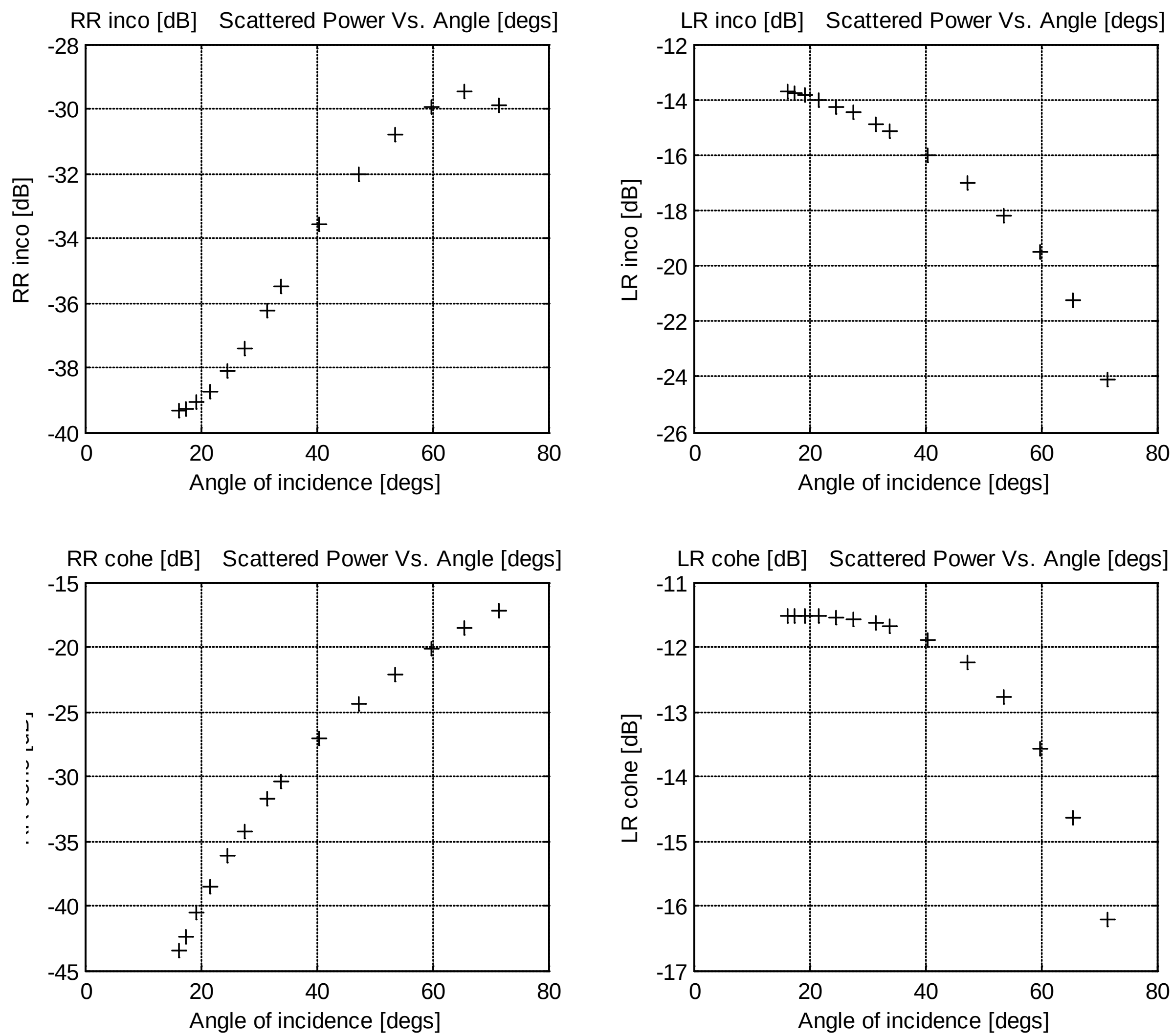

Simulator vs Leimon data

- In the Leimon experiment the instrument records the complex direct and reflected waveforms and temporal series of the waveform peaks.
  - In the following the mean reflected power normalized to the mean direct power at LR signal will be studied vs. the incidence angle
  - Different soil parameters and different vegetation conditions are investigated

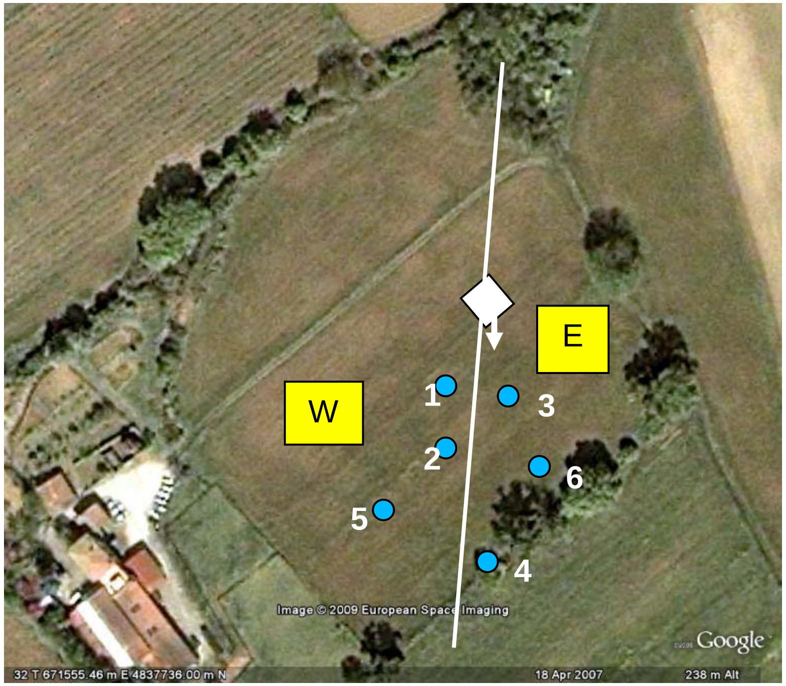

Validation: angular trend

April 8th SMC=30%

- **East field σ_Z=3cm**
- **West field σ_Z=1.75cm**

August 26th SMC=10%

- **East σ_Z=0.6 cm**
- **West σ_Z=1cm**

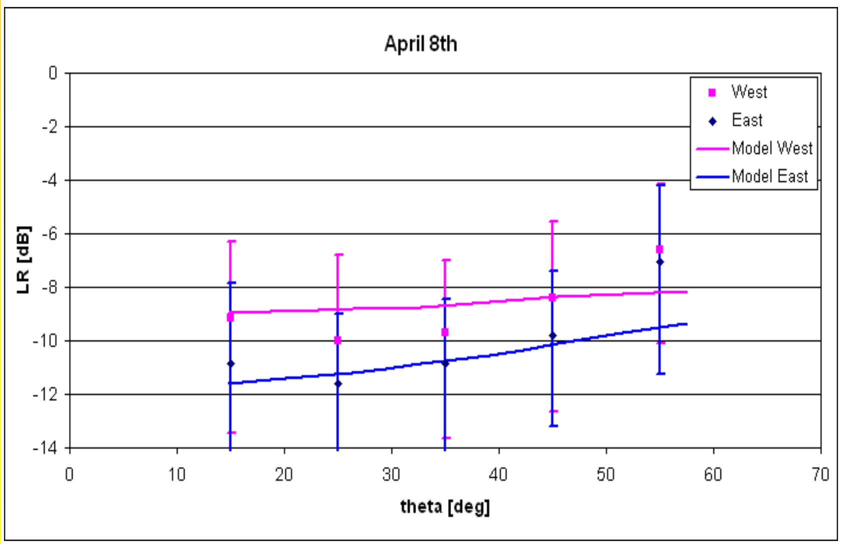

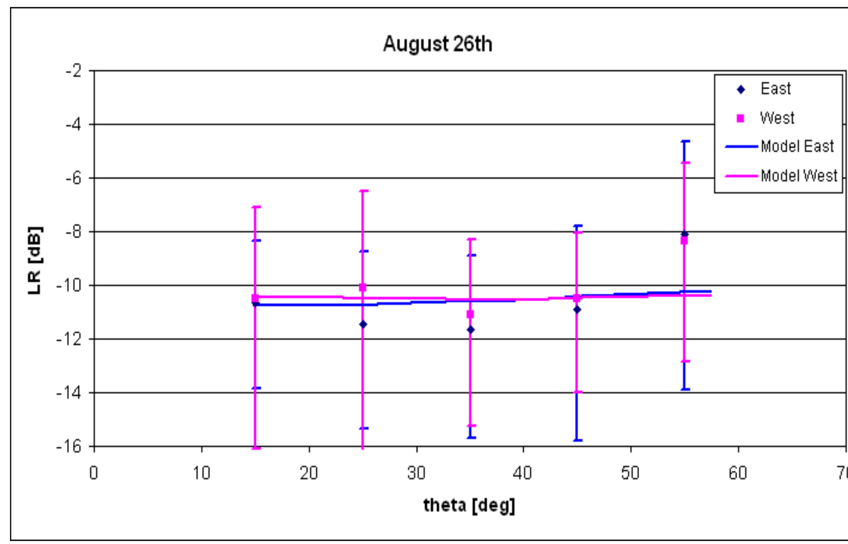

Simulator reproduces quite well LR signal at incidence angles ≤45°.

Coherent vs. incoherent: soil

April 8th SMC=30%

- **East σ_Z=3cm**

August 26th SMC=10%

- **East σ_Z=0.6 cm**

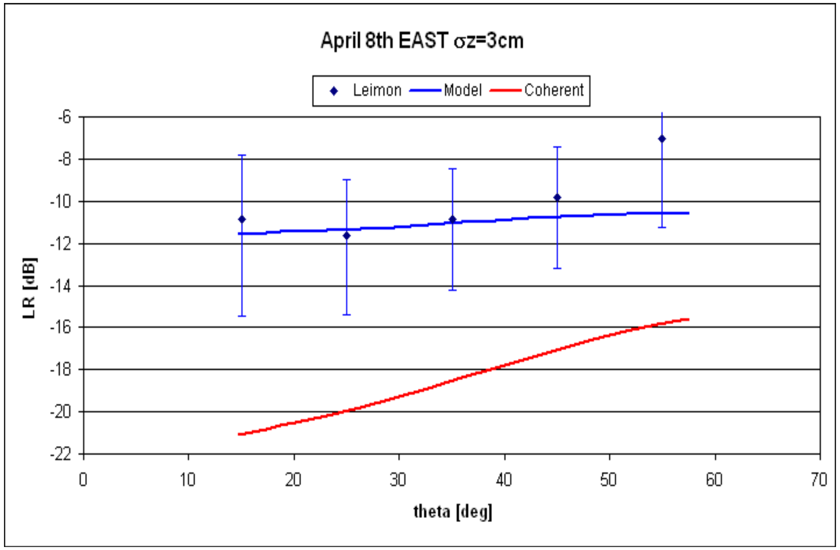

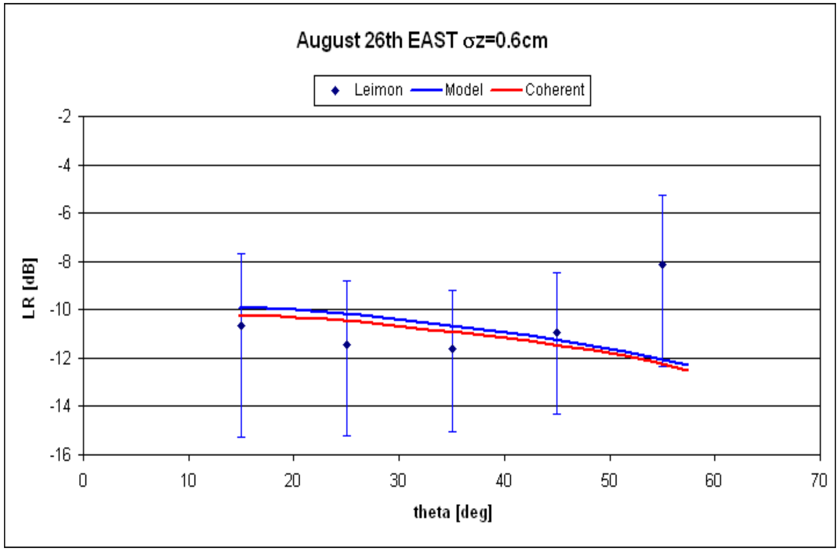

Theoretical simulations show that incoherent component contributes mainly to total signal when soil is rough.

Overall comparison

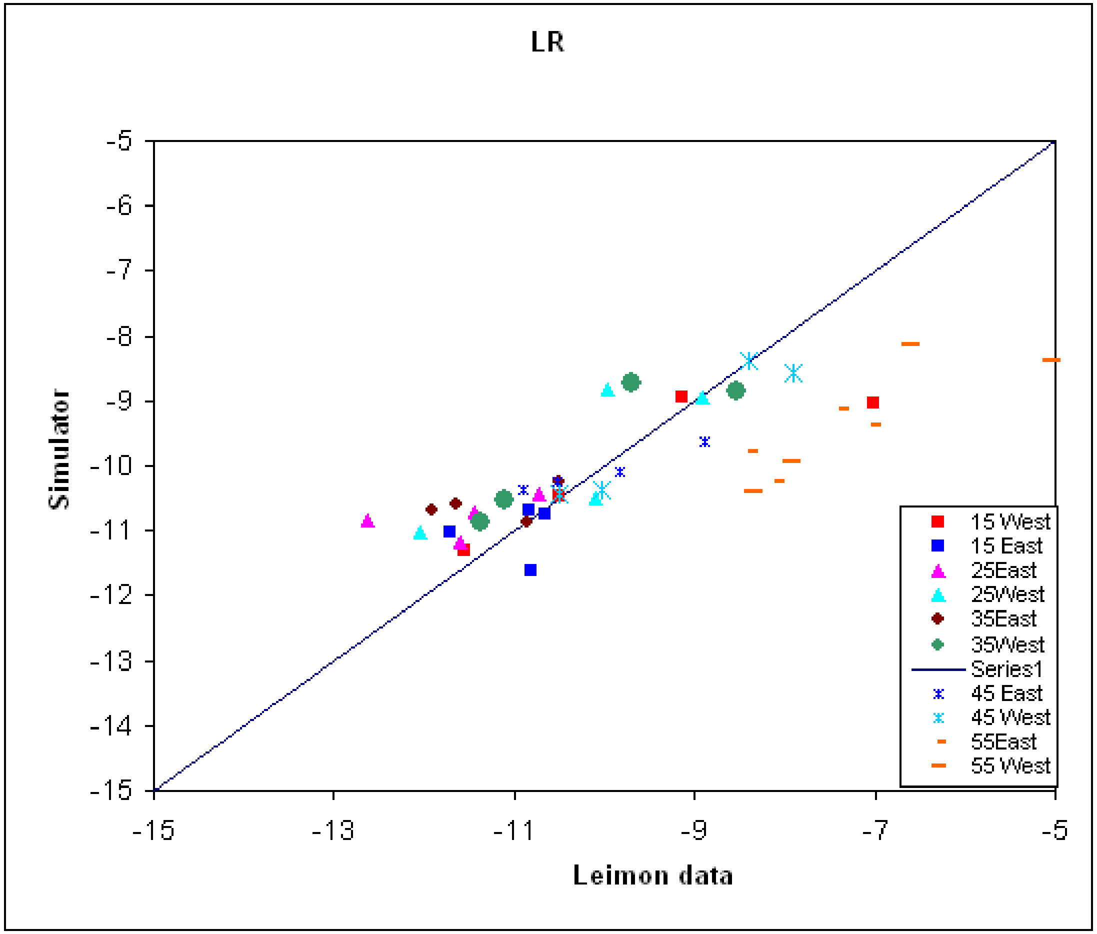

Bare Soils

10%<SMC<30%

$0.6<\sigma_z<3$cm

RMS~1 dB disregarding observations at 55°

SMC sensitivity

Power difference between soils at different SMC's

Rough soil

- April 8th SMC=30%
- May 28th SMC=17%

Smooth soil

- July 10th SMC=22%
- August 26th SMC=10%

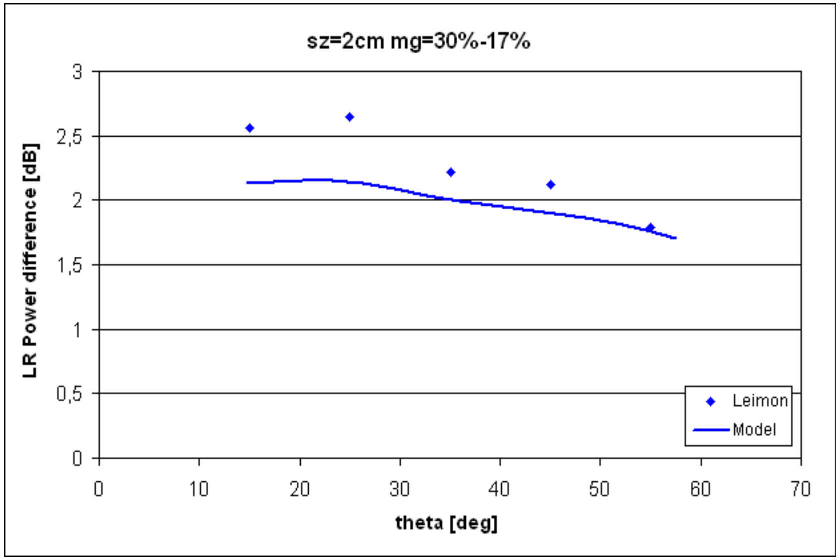

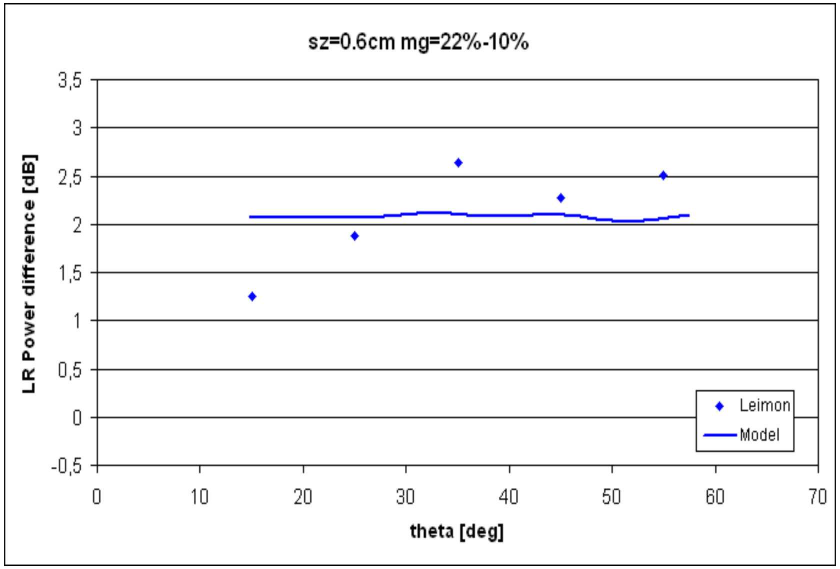

~2 dB for a 13% SMC difference

Vegetation Sensitivity

Blue=Leimon experimental data

Magenta= Simulator data

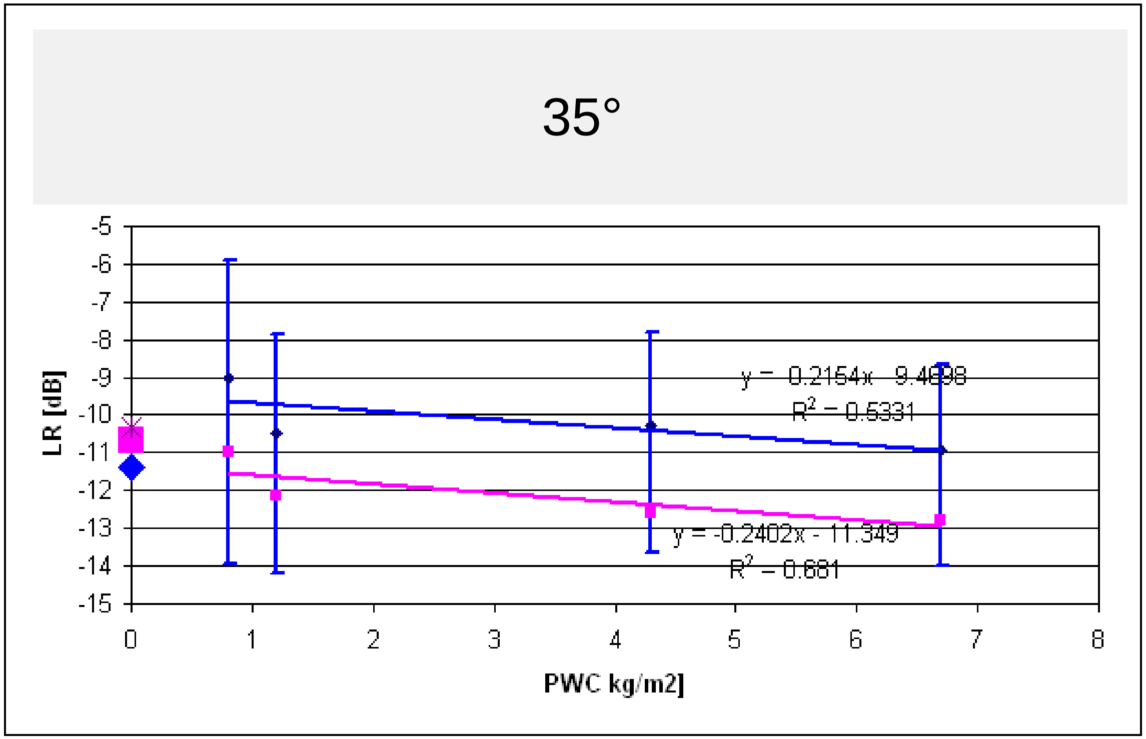

- **The model trend reproduces the measured one and it falls within the experimental error bars**
- **The sensitivity to vegetation is quite low: about 2 dB for the whole PWC range**

Coherent vs Incoherent: vegetation

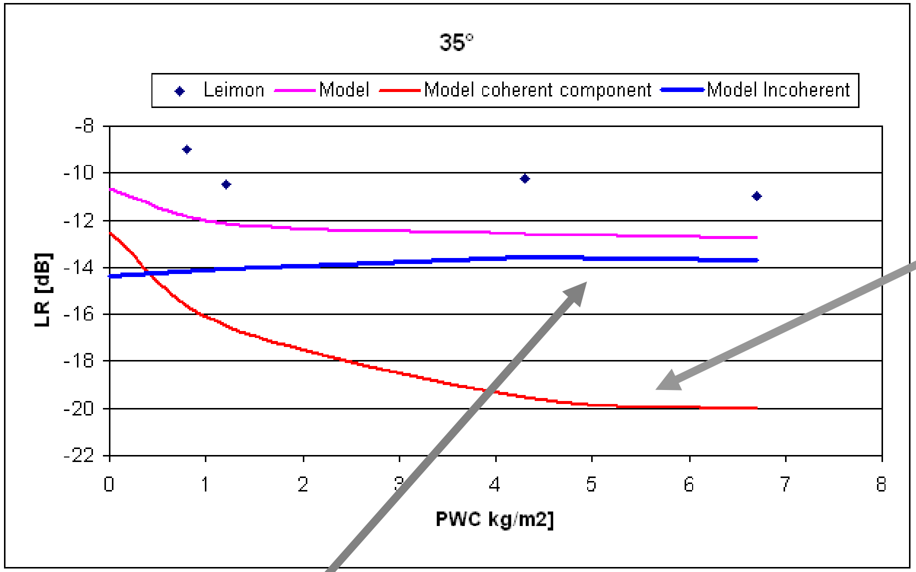

At 35 , the coherent component is attenuated by about 1 dB each 1kg/m2. This trend is in agreement with works reported in the literature for attenuation at L-band for corn plants (Ulaby et al., 1983; Jackson et al., 1982; O'Neill, 1983)

- **The Simulator predicts a quite large incoherent component which explains the saturation effect with PWC in the data.**
- **The model trend reproduces the measured one although the model is not able to reach the experimental values**

Conclusions

- **A simulator has been developed which provides DDM’s or waveforms of a GNSS-R system looking at bare or vegetated soils (LHCP and RHCP real antenna polarization)**
- **It takes in input for a given range of epochs, arbitrary receiver position/velocity, in view GPS satellite PRN code, surface properties (soil moisture, roughness, vegetation parameters).**
- **It singles out coherent and incoherent signal components coming from land with variable soil moisture, roughness, vegetation parameters.**
- **Simulator results and experimental data show a fair agreement at LR polarization and angles <45 (the antenna beamwidth)**
- **The incoherent component may be high in the ground based Leimon configuration**
- **Sensitivity to SMC is significant and well reproduced**
- **Sensitivity to Vegetation is reproduced and it is quite low because of the coherent and incoherent combination.**

Real antenna polarization

- Scattering cross section for an arbitrary combination of transmitted (incidence) and received (scattered) polarizations is provided by polarization synthesis

$$\sigma_{rt} = \frac{4\pi r^2 P^r_{rec}}{P^t_{inc}} = 4\pi \left\langle \left| \underline{\mathbf{p}}^r \cdot \underline{\underline{\mathbf{S}}}^{BSA} \underline{\mathbf{p}}^t \right|^2 \right\rangle \qquad \underline{\underline{\mathbf{S}}}^{BSA} = \begin{bmatrix} s_{vv} & s_{vh} \\ s_{hv} & s_{hh} \end{bmatrix}$$

- Nominal polarization unit vector are $\underline{\mathbf{p}}^{RHCP} = (\underline{\theta}_0 - j\underline{\phi}_0)/\sqrt{2}$ and $\underline{\mathbf{p}}^{LHCP} = (\underline{\theta}_0 + j\underline{\phi}_0)/\sqrt{2}$
- Real antenna polariz. unit vector $\underline{\mathbf{p}}^{RHCP} = \frac{\cos\theta \underline{\theta}_0 - j \underline{\phi}_0}{\sqrt{1+\cos^2\theta}}$
- SCS of "real" antennas

$$\sigma_{RR} = \frac{4\pi}{1+\cos^2\theta} \left\langle \left| \begin{bmatrix} \cos\theta \\ -j \end{bmatrix} \cdot \underline{\underline{\mathbf{S}}} \begin{bmatrix} \cos\theta \\ -j \end{bmatrix} \right|^2 \right\rangle$$

$$\sigma_{LR} = \frac{4\pi}{1+\cos^2\theta} \left\langle \left| \begin{bmatrix} \cos\theta \\ +j \end{bmatrix} \cdot \underline{\underline{\mathbf{S}}} \begin{bmatrix} \cos\theta \\ -j \end{bmatrix} \right|^2 \right\rangle$$

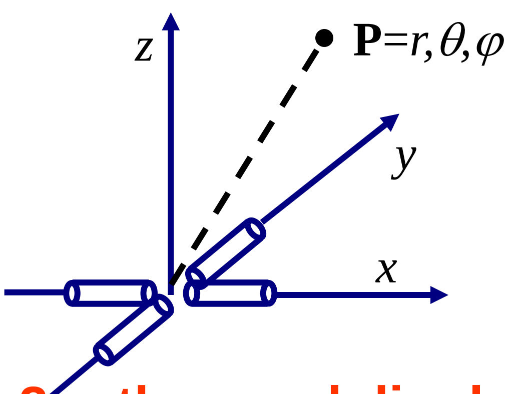

2 orthogonal dipoles π/2 phase shifted